AtCHX13 Is a Plasma Membrane K^+ Transporter[1][C][W][OA]

Jian Zhao, Ning-Hui Cheng, Christy M. Motes, Elison B. Blancaflor, Miranda Moore, Naomi Gonzales, Senthilkumar Padmanaban, Heven Sze, John M. Ward, and Kendal D. Hirschi*

United States Department of Agriculture/Agricultural Research Service Children's Nutrition Research Center, Baylor College of Medicine, Houston, Texas 77030 (J.Z., N.-H.C., M.M., N.G., K.D.H.); Plant Biology Division, Samuel Roberts Noble Foundation, Ardmore, Oklahoma 73401 (C.M.M., E.B.B.); Department of Cell Biology and Molecular Genetics, University of Maryland, College Park, Maryland 20742 (S.P., H.S.); Department of Plant Biology, University of Minnesota, St. Paul, Minnesota 55108 (J.M.W.); and Vegetable and Fruit Improvement Center, Texas A&M University, College Station, Texas 77845 (K.D.H.)

Potassium (K^+) homeostasis is essential for diverse cellular processes, although how various cation transporters collaborate to maintain a suitable K^+ required for growth and development is poorly understood. The Arabidopsis (*Arabidopsis thaliana*) genome contains numerous cation:proton antiporters (CHX), which may mediate K^+ transport; however, the vast majority of these transporters remain uncharacterized. Here, we show that AtCHX13 (At2g30240) has a role in K^+ acquisition. AtCHX13 suppressed the sensitivity of yeast (*Saccharomyces cerevisiae*) mutant cells defective in K^+ uptake. Uptake experiments using $^{86}Rb^+$ as a tracer for K^+ demonstrated that AtCHX13 mediated high-affinity K^+ uptake in yeast and in plant cells with a K_m of 136 and 196 μM, respectively. Functional green fluorescent protein-tagged versions localized to the plasma membrane of both yeast and plant. Seedlings of null *chx13* mutants were sensitive to K^+ deficiency conditions, whereas overexpression of *AtCHX13* reduced the sensitivity to K^+ deficiency. Collectively, these results suggest that AtCHX13 mediates relatively high-affinity K^+ uptake, although the mode of transport is unclear at present. *AtCHX13* expression is induced in roots during K^+-deficient conditions. These results indicate that one role of AtCHX13 is to promote K^+ uptake into plants when K^+ is limiting in the environment.

Potassium (K^+) plays an essential role in plant growth and development, affecting nutrition, membrane potential, enzyme function, and the homeostasis of many other ions (Schroeder et al., 1994; Lebaudy et al., 2007). K^+ uptake by plants exhibits a biphasic kinetic. Molecular studies in combination with membrane patch-clamp and radioisotope-flux assays suggest the presence of low-affinity voltage-gated K^+ channels, such as KAT1 (Lebaudy et al., 2007), high- and low-affinity H^+-coupled K^+ transporters (Rodriguez-Navarro and Rubio, 2006), as well as dual-affinity transporters like KUP1 (Fu and Luan, 1998; Kim et al., 1998). Perturbations in specific K^+ transporters cause alterations in leaf K^+ acquisition, root growth, and cell expansion (Gaymard et al., 1998; Rigas et al., 2001; Elumalai et al., 2002). However, many other transporters likely play important roles in plant K^+ nutrition and homeostasis.

The complete Arabidopsis (*Arabidopsis thaliana*) genome has revealed additional genes encoding cation transporter homologs (Maser et al., 2001). A database search of polytopic membrane proteins identified a list of 1,120 putative open reading frames (ORFs) encoding proteins homologous with classified transporters (Bock et al., 2006). A majority of these uncharacterized ORFs are predicted to function as secondary active transporters or H^+-coupled cotransporters (Maser et al., 2001; Ward, 2001). Among the genes encoding putative H^+-coupled transporters in Arabidopsis, approximately 44 genes encode proteins similar to Na^+/H^+ exchangers. Phylogenic analysis indicates these Arabidopsis monovalent cation:proton transporters can be divided into three families: CPA1 (NHX, eight members), NhaD (two members), and CPA2 (including CHX, 28 members; KEA, six members; Sze et al., 2004). Several CPA1 family members have been characterized extensively. For example, AtNHX1 localizes to the vacuolar membrane and can transport both Na^+ and K^+ and is also involved in pH regulation (Fukada-Tanaka et al., 2000; Venema et al., 2002; Pardo et al., 2006).

[1] This work was supported in part by the U.S. Department of Agriculture/Agricultural Research Service (under Cooperative Agreement 58–62650–6001), the National Science Foundation (NSF; grant nos. 0344350 and 020977), and the U.S. Department of Agriculture/Cooperative State Research, Education, and Extension Service (grant no. 2005–34402–17121 to K.D.H.). Work in the laboratory of J.M.W. and H.S. was supported by the NSF (grant nos. IBN–0209792 and IBN–0209788, respectively). The confocal microscope used in this study was supported by the NSF (grant no. DBI–0400580 to E.B.B.).

* Corresponding author; e-mail kendalh@bcm.tmc.edu.

The author responsible for distribution of materials integral to the findings presented in this article in accordance with the policy described in the Instructions for Authors (www.plantphysiol.org) is: Kendal D. Hirschi (kendalh@bcm.tmc.edu).

[C] Some figures in this article are displayed in color online but in black and white in the print edition.

[W] The online version of this article contains Web-only data.

[OA] Open Access articles can be viewed online without a subscription.

www.plantphysiol.org/cgi/doi/10.1104/pp.108.124248

Members of the CPA2 family are poorly defined. The plant CHX proteins have 10 to 12 membrane-spanning domains and a carboxy tail of variable length. Phylogenetic analysis indicates the CHX family can be separated into five subclades (Sze et al., 2004). Several members of subclade IV have been partially characterized, including AtCHX17 (At4g23700), AtCHX20 (At3g53720), AtCHX21 (At2g37910), and AtCHX23 (At1g05580; Cellier et al., 2004; Song et al., 2004; Sze et al., 2004; Hall et al., 2006). Many of the CHX transporters are preferentially or specifically expressed as pollen matures (Sze et al., 2004) and several are expressed in vegetative tissues. However, no pollen defects in *atchx* mutants have been described possibly due to functional redundancy. Mutant studies infer that AtCHX17, most closely related to yeast (*Saccharomyces cerevisiae*) KHA1, is an endomembrane transporter that plays a role in K^+ homeostasis (Cellier et al., 2004; Maresova and Sychrova, 2006). AtCHX20 is also an endomembrane-localized transporter that plays a critical role in osmoregulation specifically in guard cells (Padmanaban et al., 2007). AtCHX21 resides on the plasma membrane and appears to have a role in regulating xylem Na^+ concentrations and Na^+ accumulation in the leaf when the plant is under salt stress (Hall et al., 2006). The function of AtCHX23 is less clear. One study concluded this transporter affects chloroplast function and plant salt tolerance, perhaps through its role in regulation of stromal pH (Song et al., 2004); however, another study suggests a role in pollen function (Sze et al., 2004; H. Sze, unpublished data). Heterologous expression in yeast was used to show that AtCHX17 can suppress yeast endosomal defects in K^+ transport (Maresova and Sychrova, 2006), whereas AtCHX20 promotes yeast growth at low K^+ when the pH is alkaline (Padmanaban et al., 2007), suggesting a role of CHX17 in K^+ homeostasis and of CHX20 in K^+ and pH homeostasis. However, none of the previous studies analyzed directly the transport function of CHX.

Here, we have taken multiple approaches to ascertain the function of AtCHX13, a member of subclade III (Sze et al., 2004), which has not yet been studied (to our knowledge). First, we describe the growth characteristics of yeast strains expressing the transporter and provide detailed analysis of the transport kinetics of AtCHX13 in yeast. Second, we analyze the intracellular localization of AtCHX13 and the influence of various stresses on *AtCHX13* expression. Third, we show that perturbing *AtCHX13* in planta causes alterations in growth and K^+ ($^{86}Rb^+$) uptake. Collectively, these studies demonstrate that AtCHX13 localizes to the plasma membrane and has a role in mediating high-affinity K^+ uptake.

RESULTS

AtCHX13 Belongs to a Distinct Clade of the CHX Family

In a family of 28 CHX members phylogenetically separated into five subclades, AtCHX13, AtCHX14, along with AtCHX26 and AtCHX27, compose subclade III (Sze et al., 2004). None of these subclade III transporters has been experimentally characterized. Interestingly, rice (*Oryza sativa*) CHX transporters related to subclade III have not been identified (Sze et al., 2004), suggesting monocots lack these transporters. To study the function of AtCHX13, reverse transcription (RT)-PCR was used to clone the *AtCHX13* (At2g30240) cDNA. Previous studies revealed that *AtCHX13* is highly expressed in pollen grains (Sze et al., 2004). Therefore, total RNA extracted from Arabidopsis pollen grains was used to amplify the *AtCHX13* coding sequences using gene-specific primers. The *AtCHX13* cDNA consists of 2,496 nucleotides and a predicted polypeptide containing 831 amino acids (EF571901). The closely related *AtCHX14* cDNA comprises 2,490 nucleotides, which could encode a protein with 829 amino acids (EF571900; Supplemental Figure S1A; data not shown). The *AtCHX13* cDNA and deduced protein revealed substantial similarities to other AtCHX transporters: AtCHX17 and AtCHX23 (AY926473 and AY926477, respectively; Supplemental Fig. S1A). AtCHX13 shows the highest identity (71%) and similarity (84%) with AtCHX14, confirming they are products of an ancient chromosomal segmental duplication (Sze et al., 2004). In contrast, AtCHX13 shares 31% identity and 52% similarity with AtCHX17, 29% identity and 50% similarity with AtCHX23. The deduced AtCHX13 protein contains 10 predicted transmembrane domains, (Supplemental Fig. S1B). AtCHX13 does not contain a predicted organelle-targeting sequence (data not shown) and the C-terminal region did not show substantial similarity to proteins of known functions (data not shown). Computational analysis (using the TMHMM2 program) clearly indicated AtCHX13 has similar topology with the other AtCHX transporters (Supplemental Fig. S1B).

Function of AtCHX13 in K^+ Acquisition in Yeast

We detected a growth change in a yeast mutant (LMM04) expressing *AtCHX13*. LMM04 lacks several functional K^+ transporters, including TRK1, TRK2, TOK, and the endomembrane KHA1 is very sensitive to low K^+. LMM04 can only grow in medium with high levels of exogenous K^+ (Maresova and Sychrova, 2005). We confirmed that the yeast strains grew normally in medium supplemented with 200 mM KCl, whereas vector controls were not able to grow in the medium with low K^+ (Fig. 1A). Expression of *AtKAT1*, coding an inward-rectifying Arabidopsis K^+ channel (Nakamura et al., 1997), suppressed the hypersensitivity of LMM04 to lower K^+ (Fig. 1A). Surprisingly, yeast mutant cells expressing *AtCHX13* grew on medium containing low (5–20 mM) K^+ in a similar manner to *AtKAT1*-expressing cells suggesting that AtCHX13 has a role in acquiring K^+ (Fig. 1A).

To determine whether AtCHX13 could directly alter K^+ content (accumulation) in yeast, LMM04 cells expressing vector, *AtCHX13*, and *KAT1* were grown in synthetic medium (SC) with 5 mM KCl and then

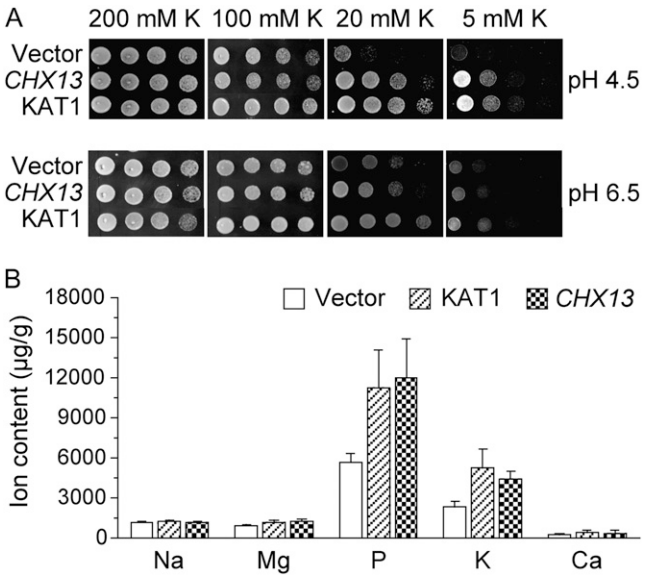

Figure 1. Functional expression of *AtCHX13* in yeast mutant LMM04. A, LMM04 cells expressing vector, *AtCHX13*, or *KAT1* were grown overnight in selection medium (SC-Ura) supplemented with 100 mM KCl. Cultures were brought to a uniform cell density and 5-fold serial dilutions were spotted on SC-Ura medium at various pHs and varying concentrations of KCl. Photos were taken after 4 d of growth at 30°C. B, Cation content of LMM04 yeast expressing empty vector, *AtCHX13*, or *KAT1*. All yeast strains were grown overnight in SC medium plus 100 mM KCl and then harvested and washed with K^+-free medium. Two hundred microliters of each cell culture was then transferred to 5 mL of low K^+ medium (supplemented with 5 mM KCl). After overnight growth, yeast cultures were collected onto membranes and washed three times with water for inductively coupled plasma analysis. Data are presented as means ± SD (n = 5). One-way ANOVA with Tukey's multiple comparison procedures was used for pairwise comparisons.

subjected to ion analysis using inductively coupled plasma-mass spectroscopy. The resulting accumulation profile of several elements (calcium [Ca], K, magnesium [Mg], phosphorus [P], sodium [Na]) was determined in these yeast strains (Lahner et al., 2003). As shown in Figure 1B, K^+ content in *AtKAT1*- and *AtCHX13*-expressing cells was significantly higher than the vector controls. Interestingly, P levels were also significantly higher in the *AtKAT1*- and *AtCHX13*-expressing cells, whereas the other ions were not different than the controls. Thus, an increase in yeast growth caused by AtCHX13 is accompanied by K^+ accumulation.

To further characterize AtCHX13, we expressed the transporter in yeast strains lacking only functional TRK1 and TRK2 (Supplemental Fig. S2). AtCHX13 and AtKAT1 restored growth of mutants (*trk1trk2*) at low K^+ (1–5 mM) when compared to vector controls. For both LMM04 (Fig. 1) and *trk1trk2* (Supplemental Fig. S2), the difference between controls and both *AtKAT1*- and *AtCHX13*-expressing cells was most pronounced at pH 4.5.

AtCHX13 Mediates High-Affinity K^+ Uptake

To further test AtCHX13 function in K^+ uptake, we expressed the full-length cDNA in the yeast mutant strain LMM04 (where the phenotype was most robust) and measured K^+ uptake using radioactive rubidium (^{86}Rb) as a tracer. For simplicity, we assumed that ^{86}Rb mimics K^+ influx and later directly tested this assumption (see below). We analyzed ^{86}Rb uptake as a function of time in LMM04 vector controls and cells expressing *AtCHX13* or the K^+ channel *AtKAT1*. To identify experimental conditions under which the initial rate of K^+ uptake could be measured, time course analysis of K^+ uptake was performed at 0.02 mM (Fig. 2A) and 20 mM (Fig. 2B) external K^+. Under both conditions, uptake was linear for at least 5 min and both *AtCHX13*- and *AtKAT1*-expressing cells had significantly higher K^+ uptake rates compared to vector controls. Yeast cells expressing *AtCHX13* had higher K^+ uptake at low (0.02 mM) K^+ concentrations compared to *AtKAT1*-expressing cells, whereas at 20 mM K^+, *AtKAT1*-expressing cells demonstrated increased uptake compared to *AtCHX13*-expressing cells.

Kinetic analysis was performed for K^+ uptake by yeast cells expressing *AtCHX13* or *AtKAT1*. Initial uptake rates (within the first 5 min of K^+ addition) were plotted as a function of external K^+ concentration (Fig. 2C). K^+ uptake by *AtCHX13*-expressing yeast was near maximum at below 1 mM, indicating high-affinity K^+ uptake. Uptake in *AtKAT1*-expressing yeast did not show saturation up to 5 mM K^+, indicating a lower affinity for K^+ (Fig. 2C). After subtracting the K^+ uptake rate from vector controls, reciprocal plots for *AtCHX13*-expressing yeast cells showed a K_m for K^+ of 136.4 μM and V_{max} of 14.4 nmol h^{-1} 10^{-7} cells (Fig. 2D). Given that AtKAT1-mediated K^+ uptake did not show saturation in the substrate range measured, we were unable to estimate a K_m for AtKAT1.

To establish that Rb^+ uptake by *AtCHX13*-expressing cells is an accurate indicator of K^+ uptake kinetics, we measured Rb^+ uptake at 5 min in assay solutions containing 0.02, 2.0, and 20 mM of RbCl and KCl. The uptake rates were virtually identical in the K^+- and Rb^+-containing uptake solutions (data not shown), an indicator that Rb^+ flux is mimicking K^+ uptake.

AtCHX13-mediated K^+ uptake assays at 0.02 mM K^+ was blocked by cesium (Cs^+) and Na^+ (Fig. 2E). Cs^+ inhibited the high-affinity uptake of K^+ significantly at concentrations above 1 mM. Similarly, K^+ uptake in *AtCHX13*-expressing yeast cells was inhibited when greater than 1 mM NaCl was present (Fig. 2E). These results suggest that Na^+ and Cs^+ block K^+ transport by competing for the same cation-binding site. Cs^+ inhibits K^+ uptake through most K^+ channels and some other transporters (Hedrich and Schroeder, 1989; Tester, 1990). Early studies demonstrated that K^+ uptake by plant roots is inhibited by millimolar concentrations of NaCl (for review, see Epstein, 1972).

To probe the mode of AtCHX13-mediated K^+ uptake in yeast, we tested the effect of pH and carbonyl cyanide *m*-chlorophenylhydrazone (CCCP; Fig. 2F). AtCHX13-mediated uptake at 20 μM external K^+ was higher at pH 4.3 relative to pH 7.5. Furthermore,

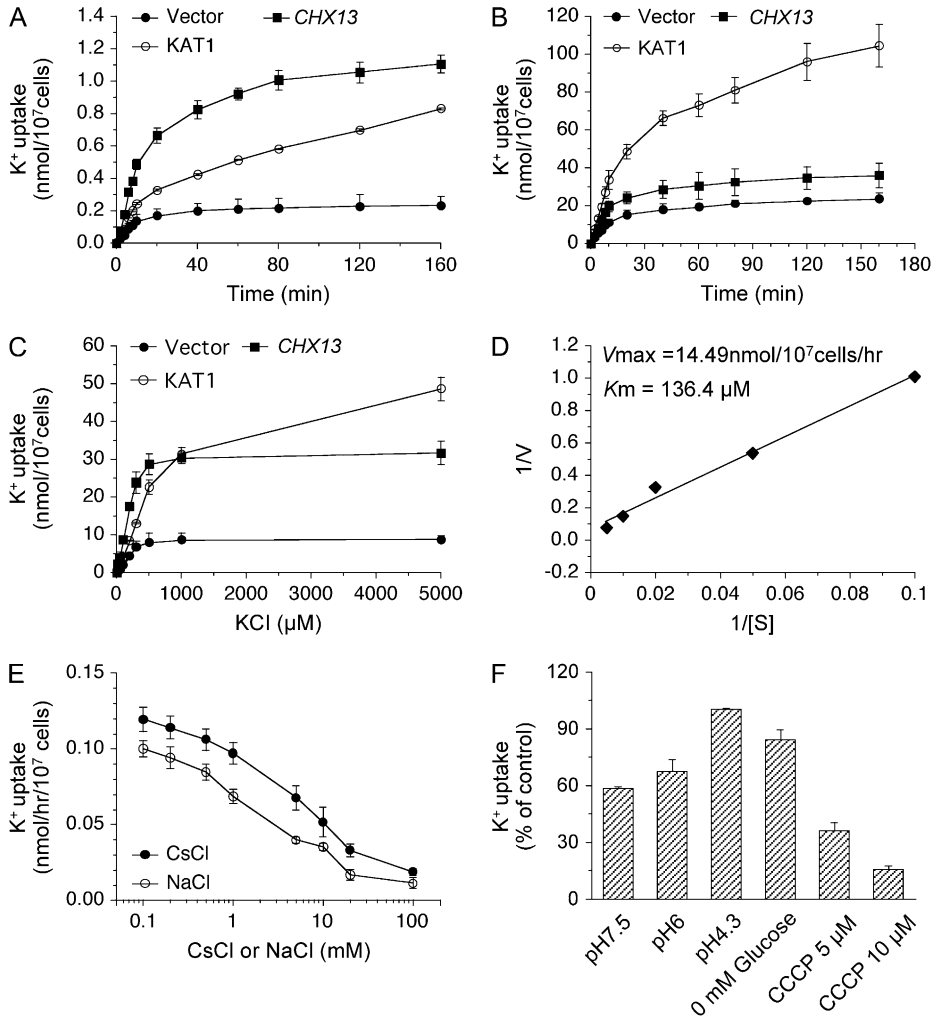

Figure 2. K^+ (^{86}Rb) uptake in yeast cells expressing *AtCHX13* and *KAT1*. Yeast cells were grown in SC medium depleted of K^+ for 5 h prior to $^{86}Rb^+$ uptake. At least three independent experiments were performed with duplicates for each treatment (data points represent means ± SD). A and B, Time course of K^+ (^{86}Rb) uptake at 0.02 (A) and 20 mM (B) external K^+. C, The uptake rate in the range of 0 to 5,000 μM K^+ at 5 min. D, Lineweaver-Burk plot of AtCHX13-mediated K^+ (^{86}Rb) uptake. AtCHX13-mediated K^+ uptake was obtained by subtracting the uptake in vector control expressing cells from that in the *AtCHX13*-expressing yeast. [S], K^+ concentration (μM); V, K^+ uptake rate (nmol h^{-1} 10^{-7} cells). E, Effect of CsCl and NaCl on AtCHX13-mediated K^+ (^{86}Rb) uptake at 20 μM external [K^+]. CsCl or NaCl concentrations are detailed in "Materials and Methods." Except where noted, all uptakes were done with 10 mM Glc, at 5 min and at pH 4.3. F, Effects of pH, Glc, and CCCP on AtCHX13-mediated K^+ (^{86}Rb) uptake at 20 μM external [K^+]. All assays were conducted with 10 mM Glc unless otherwise indicated. The pH was buffered with 5 mM MES-Tris. CCCP was added to the yeast cells in uptake buffer (pH 4.5) 5 min prior to K^+ and ^{86}Rb tracer addition. Glc was excluded in one assay (0 mM Glc) at pH 4.5. Data show uptake at 5 min and 100% activity (pH 4.3, 20 μM external K^+) is 0.133 nmol h^{-1} 10^{-7} cells.

CCCP, a protonophore, reduced K^+ uptake. Glc had little to no effect, indicating that energy from carbon metabolites was not limiting. These results suggest that K^+ uptake is dependent on a pH gradient (acid outside).

AtCHX13-GFP Localized to the Plasma Membrane

To determine the subcellular localization, a fusion of AtCHX13 with GFP at the C terminus (AtCHX13-GFP) was constructed. The function and localization of AtCHX13-GFP was tested in yeast (Supplemental Fig. S3). The addition of GFP did not abolish the function of AtCHX13, although the fusion protein showed weaker ability to restore yeast growth than CHX13 or KAT1. In yeast, AtCHX13-GFP was predominantly localized peripherally, consistent with plasma membrane localization (Fig. 3A) and in contrast to the uniform cytoplasmic labeling in cells expressing *GFP* (Fig. 3B). In plant cells, *AtCHX13-GFP* was transiently expressed under the control of the cauliflower mosaic virus 35S promoter in tobacco (*Nicotiana tabacum*) and onion (*Allium cepa*) epidermal cells (Fig. 3, D and E). When imaged by confocal microscopy, the localization pattern of AtCHX13-GFP was markedly different from that of soluble GFP. A maximal projection image of several confocal optical sections of cells expressing soluble GFP revealed an extensive network of cytoplasmic strands, which is characteristic of cytoplasmic localization (Fig. 3C). On the other hand, *AtCHX13-GFP*-expressing cells displayed intense fluorescence confined to the cell periphery. Maximal projection images of a series of confocal optical sections revealed uniform GFP labeling along the cell surface and the absence of any fluorescent strands. These features are strongly indicative of the plasma membrane localization of AtCHX13 (Fig. 3, D and E). To exclude the possibility that AtCHX13-GFP localized to the cell wall, onion cells were plasmolyzed by treatment with 1 M Suc. The fluorescence in the plasmolyzed cells detached from the cell wall, confirming that the AtCHX13-GFP signal was not from the cell wall or the apoplastic space between the cells (Fig. 3E). Our plasmolysis experiment also allowed us to distinguish between plasma membrane and tonoplast labeling. In fully differenti-

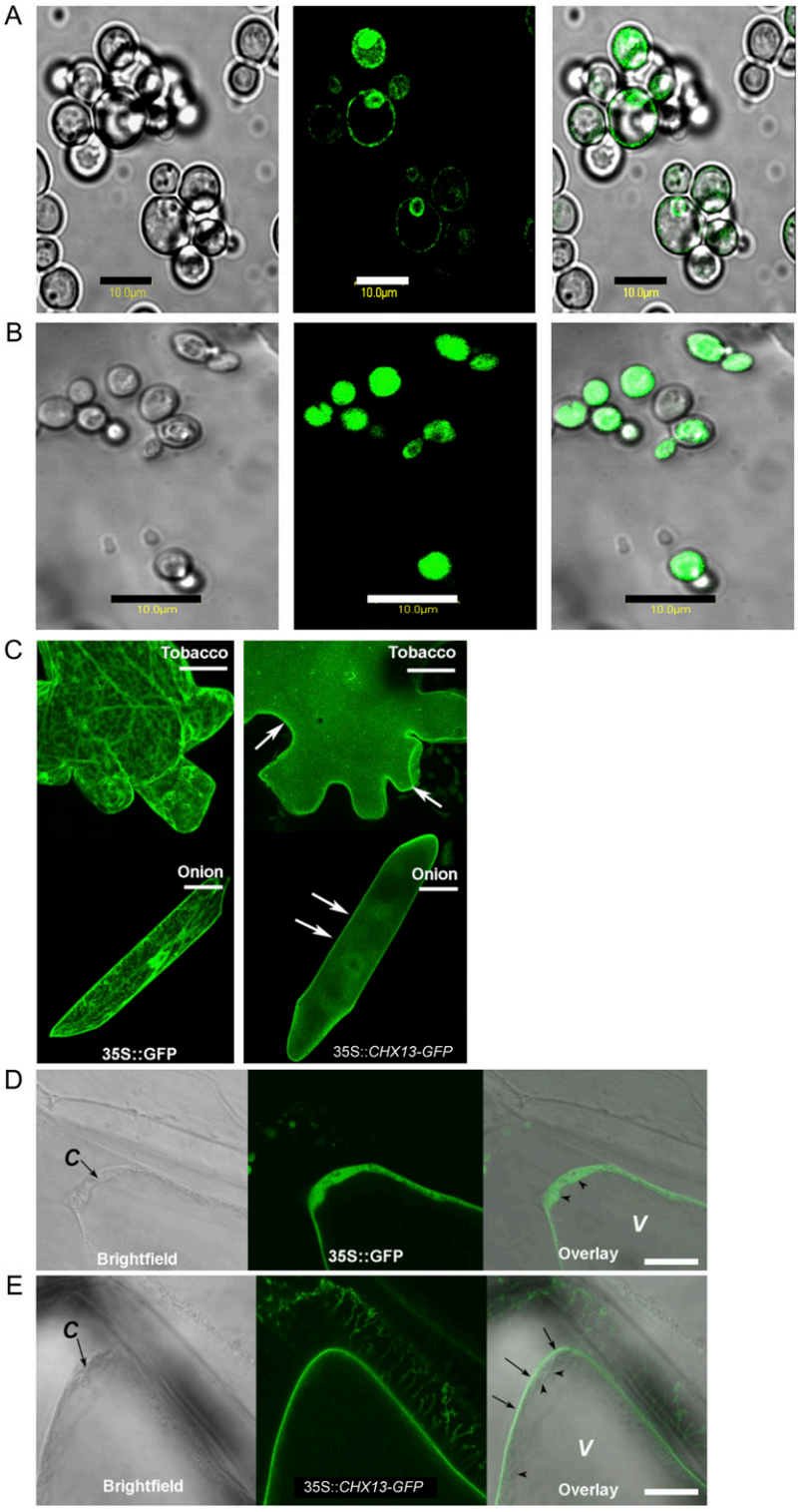

Figure 3. Cellular localization of AtCHX13. A and B, Single confocal optical sections of yeast cells expressing *AtCHX13-GFP* (A) and free *GFP* (B) driven by GPD promoter. Left, middle, and right images are fluorescent, bright-field, and merged images, respectively. Bars = 10 μm. C, Onion (bottom) and tobacco (top) epidermal cells expressing 35S::*GFP* (left) and 35S::*AtCHX13-GFP* (right) constructs. Cells expressing 35S::*GFP* are characterized by numerous fluorescent strands, which is typical of cytoplasmic localization. Cells expressing 35S::*AtCHX13-GFP* show intense fluorescence along the cell periphery (arrows) and uniform labeling at the surface, resembling plasma membrane localization. Images are projections of 30 to 50 optical sections taken at 0.5-μm intervals. Bar = 20 μm. D and E, Single optical sections of onion epidermal cells expressing 35S::*GFP* (D) or 35S::*AtCHX13-GFP* (E) plasmolyzed with 1 M Suc. A region of the cell where the cytoplasm is thicker is shown to clearly distinguish between the plasma membrane and tonoplast localization. The cytoplasm (c) can be detected based on its granular appearance in the bright-field images. Note that fluorescence of GFP is located throughout the cytoplasm (D), whereas AtCHX13-GFP fluorescence is restricted to a thin line along the surface of the cytoplasm (E) corresponding to the plasma membrane (arrows). The arrowheads in the overlay images (D and E) correspond to the location of the tonoplast. Note that absence of AtCHX13-GFP fluorescence in this region. Bar = 100 μm.

ated cells, such as the onion inner epidermal cells used here, a large central vacuole typically pervades a large portion of the cell leaving only a thin layer of cytoplasm compressed toward the edge of the cell. This often makes it difficult to distinguish whether GFP signal originates from the plasma membrane, tonoplast, or cytoplasm. We therefore imaged regions of the cell where we could readily visualize the cytoplasm. In a plasmolyzed onion cell expressing 35S::*GFP*, a slightly thickened region of the cytoplasm could be seen using bright-field optics. A corresponding fluorescence image showed that GFP signal was

uniformly distributed within this cytoplasmic domain (Fig. 3D). In contrast, *AtCHX13-GFP*-expressing cells showed intense fluorescence originating from a thin layer along the outer edge of the cytoplasm, confirming plasma membrane, but not tonoplast, localization (Fig. 3E).

AtCHX13 Is Expressed in Seedlings and in Response to K^+ Fluctuations

Microarray and preliminary promoter-driven GUS results suggest that *AtCHX13*, like 13 other *AtCHX* genes, is expressed during pollen development (https://www.genevestigator.ethz.ch; Sze et al., 2004). To more systematically characterize *AtCHX13* expression, we monitored expression using RT-PCR and *AtCHX13* promoter-driven GUS activity. Using northern analysis, *AtCHX13* showed little or no expression in seedlings given a variety of ionic stresses, including increased and decreased levels of Na^+, K^+, and Ca^{2+}. Using RT-PCR, we confirmed microarray results that *AtCHX13* was expressed weakly in several plant tissues, including roots (Fig. 4A). Using RT-PCR to determine expression in seedlings, we showed that *AtCHX13* expression could be detected 1 d after plants were depleted of K^+ (Fig. 4B). When plants were exposed to higher levels of K^+ (100 mM), *AtCHX13* expression could be detected in seedlings after 1 d, but expression appeared to dissipate at day 2 and beyond.

To verify the expression results, promoter-driven GUS activity was determined. Due to low expression levels in vegetative tissues, *AtCHX13*::GUS activity could only be reproducibly measured in pollen when plants were grown on standard medium (J. Zhao and K. Hirschi, unpublished data; Sze et al., 2004). When K^+ was limiting, *AtCHX13*::GUS root expression increased compared to lines grown in normal medium (10 mM K^+; Fig. 4C). *AtCHX13* promoter-GUS expression and RT-PCR data indicated *AtCHX13* expression is enhanced in response to decreased K^+ conditions.

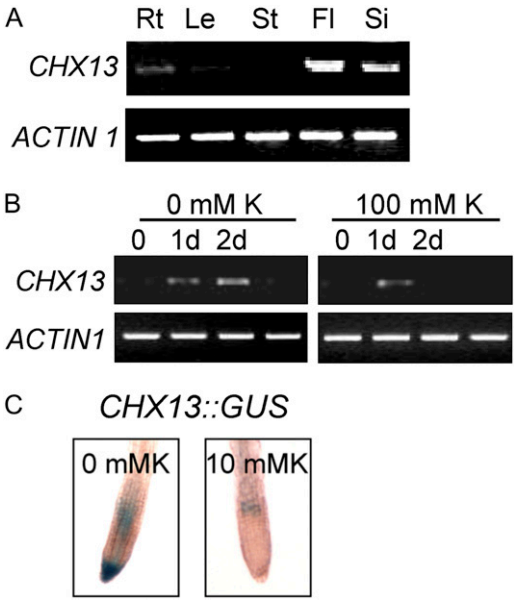

Figure 4. *AtCHX13* expression. A, Vegetative and reproductive organs. Total RNA was isolated from roots (Rt), leaves (Le), and stems (St; from 3-week-old plants), flowers (Fl), and siliques (Si; from 4-week-old plants), reverse transcribed, and subjected to RT-PCR. ACTIN1 was used as internal standard. Images shown represent results obtained from three independent amplification reactions. B, RT-PCR analysis of *AtCHX13* expression when seedlings were grown on high and low K^+. RT-PCR analysis of *AtCHX13* expression. One-week-old Col-0 seedlings were transferred to 0.5× Murashige and Skoog medium supplemented with 100 mM KCl or to modified 0.5× Murashige and Skoog with low levels of K^+ (the agar provides the medium with approximately 0.4 mM K^+). The seedlings were collected at specified time points as indicated for RNA isolation. The samples were then analyzed as described in A. ACTIN1 was used as internal control. C, *AtCHX13*::GUS lines were grown on 0.5× Murashige and Skoog plate for 9 d and then transferred to 0.5× Murashige and Skoog containing either no K^+ or with 10 mM K for 2 d prior to GUS staining. [K^+] was removed (0 mM K) by replacing KNO_3, KH_2PO_4, and KI with BTP-NO_3, NaH_2PO_4, and NaI, respectively.

Altered Expression of *AtCHX13* in Plants

To study the function of AtCHX13 in plants, we obtained two independent T-DNA insertional lines for *atchx13* (Fig. 5A). Homozygous lines were identified and the positions of the T-DNA insertions were confirmed by sequencing (Fig. 5A). Using RT-PCR, no *AtCHX13* transcripts could be reverse transcribed from total RNA isolated from the mutant flowers (Fig. 5B). The *atchx13* lines showed no obvious morphological or growth defects compared to control plants under standard growth conditions (data not shown).

Additional attempts to alter *AtCHX13* expression were made by constitutive expression of the ORF in Arabidopsis (in the Columbia [Col-0] background). In the 35S::*AtCHX13* lines, PCR analysis showed augmented basal level of native gene expression (Fig. 5C). Despite the increased amount of *AtCHX13* transcripts in these lines, no change in plant growth or development was detected when the plants were grown in standard conditions (data not shown).

Phenotypes of *atchx13* Lines

The maintenance of K^+ homeostasis is important for stress responses (Marschner, 1995). The observations that the expression of *AtCHX13* was induced in seedlings grown under low K^+ conditions and that *AtCHX13* expression in yeast mediated K^+ transport suggested that AtCHX13 may function in K^+ uptake during K^+ deficiency. Under standard growth conditions (0.5× Murashige and Skoog medium containing about 10 mM K^+) *atchx13* mutants and 35S::*AtCHX13* seedlings grew similarly to control lines (Fig. 6A; Supplemental Fig. S4A). However, when these lines were germinated and grown on low K^+ medium at varying pH values, *atchx13* lines displayed obvious

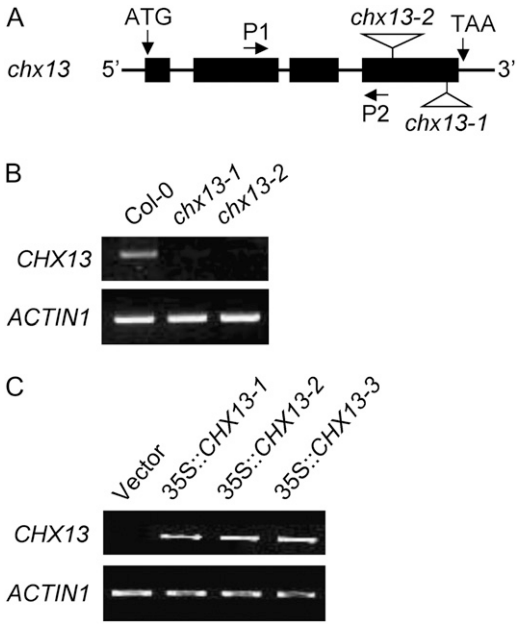

Figure 5. *AtCHX13* T-DNA insertion and transgenic lines. A, Identification of *AtCHX13* insertion lines. The positions of two independent T-DNA insertional mutants for AtCHX13 are shown. Lines *atchx13-1* and *atchx13-2* correspond to SALK lines SALK_095075 and SALK_023605, respectively. Black boxes show exons and lines between them show introns. Arrows labeled with P1 and P2 above and below black boxes show forward and reverse primers used for RT-PCR analysis, respectively. B, Absence of transcripts in T-DNA insertion mutants. RT-PCR was performed from RNA extracted from flowers of wild-type and *atchx13* lines. ACTIN1 expression was used as an internal control. C, Characterization of *AtCHX13* expression in *chx13* mutants. F3 lines of homozygous 35S::*AtCHX13* in Col-0 were used to examine gene expression. Two-week-old seedlings were harvested for RNA extraction and RT-PCR analysis. Transgenic Col-0 plants expressing the vector alone were used as a control and ACTIN1 expression was used as an internal standard.

growth phenotypes when compared to controls. Specifically, the *atchx13* lines grew more slowly and appeared to have more leaf chlorosis and bleaching (Fig. 6, B–D; Supplemental Fig. S4A). The sensitivity of *atchx13* lines to limited K^+ is obvious at low pH (4.3); however, this sensitivity is not pH dependent as some sensitivity is also observed at pH 7.5. Measurements of total chlorophyll and fresh-weight analysis in these lines reflect the growth differences (Fig. 6, E–H). That is, the *atchx13* lines displayed reduced chlorophyll content and biomass. The transgenic lines that expressed high levels of *AtCHX13* were more robust than control lines in these growth conditions (Fig. 6, A–F).

^{86}Rb uptake kinetics of 35S::*AtCHX13*, and wild-type (Col-0) seedlings were directly analyzed by measuring time- and concentration-dependent $^{86}Rb^+$ uptake into roots of K^+-starved plants. The initial uptake of $^{86}Rb^+$ was linear in all lines up to 20 min, with uptake being dramatically higher for the 35S::*AtCHX13*-expressing lines than control mutant lines (Fig. 7). Concentration-dependent $^{86}Rb^+$ uptake was subsequently measured at 10-min intervals at different external K^+ concentrations. Uptake rates for $^{86}Rb^+$ revealed a significant difference between vector control and 35S::*AtCHX13* lines at low K^+ concentrations (0.02 mM K^+; Fig. 7, A and B). The *atchx13* mutants showed uptake at 0.02 mM K^+ lower than controls (data not shown). At high K^+ concentrations (20 mM), the difference in uptake kinetics could not be resolved between vector control and the lines with enhanced *AtCHX13* expression (Fig. 7B). The influx at 20 mM K^+ was similar in all lines tested. In *atchx13* lines, $^{86}Rb^+$ uptake was slightly reduced compared to controls when K^+ was limiting (0.02 mM K^+), but was similar to controls at higher K^+ levels (Supplemental Fig. S5).

To attempt to measure the uptake rate of K^+ ($^{86}Rb^+$) by AtCHX13 in plants, the difference between the uptake rates of vector controls and 35S::*AtCHX13* was measured. A plot of the difference in uptake rates, as a function of K^+ concentration, approximates a saturable system with a K_m of 196 μM and V_{max} of 188.7 nmol g^{-1} h^{-1} (Fig. 7, C and D).

We measured $^{86}Rb^+$ uptake in 35S::*AtCHX13* lines under different pH conditions and in the presence of the protonophore CCCP (Fig. 7E). In a manner similar to the yeast cells expressing *AtCHX13*, optimal uptake was measured at acidic pH conditions and the protonophore inhibited K^+ uptake in these whole-plant experiments. Results suggest K^+ uptake is dependent on a pH or electrochemical gradient.

DISCUSSION

The ability of plants to grow and develop under myriad nutrient and environmental conditions appears to depend on multiple transporters to sustain K^+ homeostasis. In spite of numerous pathways used by plants for K^+ uptake, including channels and cotransporters, we demonstrate here that a distinct member of the *CHX* gene family has a role in supporting growth under K^+-deficient conditions.

AtCHX13 Function

Unlike CHX20 and CHX17, which have been localized to endomembranes (Maresova and Sychrova, 2006; Padmanaban et al., 2007) in plants and in yeast, we demonstrate here that AtCHX13 localizes to both yeast and plant plasma membranes. Several lines of evidence support its role in facilitating K^+ uptake at the plasma membrane: (1) *AtCHX13* can suppress yeast mutants defective in K^+ uptake (Figs. 1 and 3; Supplemental Fig. S2); (2) *AtCHX13*-expressing yeast showed increased K^+ (^{86}Rb) uptake and K^+ content compared to vector controls (Fig. 2); (3) in Arabidopsis, *AtCHX13* expression was responsive to the K^+-deficient conditions (Fig. 4); (4) T-DNA insertional mutants defective in *AtCHX13* expression demonstrate perturbed growth in response to K^+ starvation;

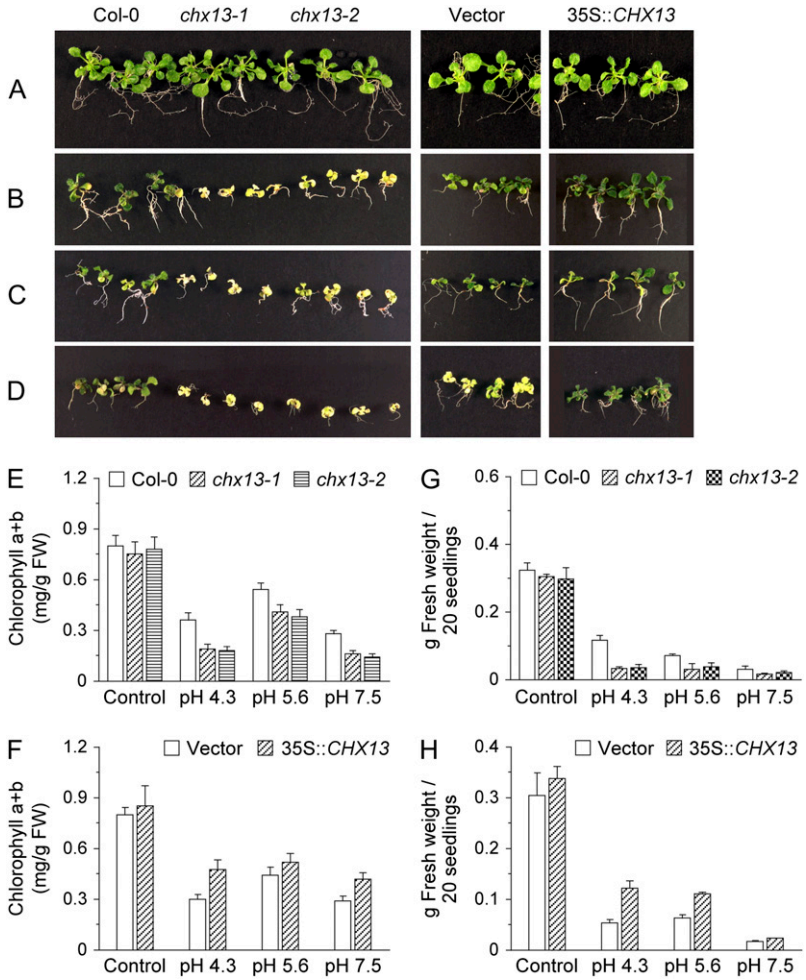

Figure 6. Differential K^+ sensitivity of Arabidopsis lines with altered *AtCHX13* expression. K^+ sensitivity of control lines (Col-0 and empty vector-expressing line), *chx13-1* and *chx13-2* mutants, and 35S::*AtCHX13* transgenic lines (in Col-0) were germinated and grown in 0.5× Murashige and Skoog medium or modified 0.5× Murashige and Skoog medium containing 2 mM K^+ at different pHs. Images shown are representative of 3-week-old plants from at least three independent experiments. Chlorophyll *a*/*b* levels and fresh weights were measured at day 25. Data are presented as means ± SD. Three independent assays were performed with duplicates for each treatment. One-way ANOVA with Tukey's multiple comparison procedures was used for pairwise comparisons. A, Seedlings grown on 0.5× Murashige and Skoog containing 10 mM K^+ at pH 5.6. B to D, Seedlings grown on modified 0.5× Murashige and Skoog containing no added K^+ (estimate 0.4 mM K^+) at pH 4.3 (B), 5.6 (C), or 7.5 (D). E and F, Chlorophyll *a*/*b* content in *atchx13* (E) or in 35S::*AtCHX13* lines (F) grown on modified 0.5× Murashige and Skoog containing no added K^+ (estimate 0.4 mM K^+) at different pH values. G and H, Biomass (in fresh weight) of *atchx13* (G) or 35S::*AtCHX13* lines (H) grown on modified 0.5× Murashige and Skoog containing no added K^+ (estimate 0.4 mM K^+) at different pH values. [See online article for color version of this figure.]

and (5) plants with increased *AtCHX13* expression showed increased rates of ^{86}Rb uptake relative to plants harboring vector only (Fig. 7).

K^+ uptake in plant roots displays biphasic kinetics (Epstein, 1972; Marschner, 1995). High-affinity uptake occurs in the low [K^+] range (1–200 μM), whereas low-affinity uptake takes place in the high [K^+] range (1−50 mM). The high-affinity system, with the tight coupling of the proton motive force, can function in transporting K^+ against its electrochemical potential gradient. K^+ (^{86}Rb) uptake into yeast (K_m = 136.4 μM) or plants (K_m = 196 μM) with *AtCHX13* expression suggest a high-affinity K^+ transporter because uptake above the background was increased at 20 μM K^+, but was not altered at 20 mM K^+. The K_m determined for K^+ uptake mediated by AtCHX13 in yeast and plants is similar. Minor differences may be a function of membrane potential, pH, or the presence/absence of modifying proteins (Hedrich and Schroeder, 1989; Kochian et al., 1993; Fu and Luan, 1998). In both expression systems, AtCHX13 appears to mediate high-affinity K^+ uptake.

At present, the mode of K^+ uptake is unclear. AtCHXs characterized so far are thought to mediate K^+ uptake into endomembrane compartments via a cation/proton exchange mechanism (Cellier et al., 2004; Padmanaban et al., 2007). To our knowledge, AtCHX13 is the first characterized plasma membrane-localized CHX that facilitates uptake of K^+ with high affinity. AtCHX21 has also been localized to the PM; however, the transport activity of this protein has not been tested (Hall et al., 2006). AtCHX13-mediated K^+ uptake is enhanced by a proton electrochemical gradient (acidic outside; Figs. 1, 2, and 7), suggesting the protein may operate as a K^+/H^+ symporter instead of an antiporter (K^+ influx for H^+ efflux). However, we were unable to measure currents in oocytes expressing either *AtCHX13* or the closely related *AtCHX14* (data not shown) in initial tests. The possibility of AtCHX13 behaving like an influx channel is also considered. The sequence of CHX shares little homology to known K^+ channels, and specific inhibitors of voltage-gated K^+ channels, such as TEA and Ba^{2+}, inhibit AtKAT1 function in yeast cells (Anderson et al., 1992), but did not perturb yeast growth in *AtCHX13*-expressing cells (data not shown). Yet AtCHX13, like KAT1, restored growth to yeast mutants defective in K^+ uptake pathways. AtCHX13 mediated relatively high-affinity K^+ uptake, similar to some KUP/HAK/KT K^+ transporters (Very and Sentenac, 2003). It is possible that AtCHX13 protein has multiple catalytic modes at

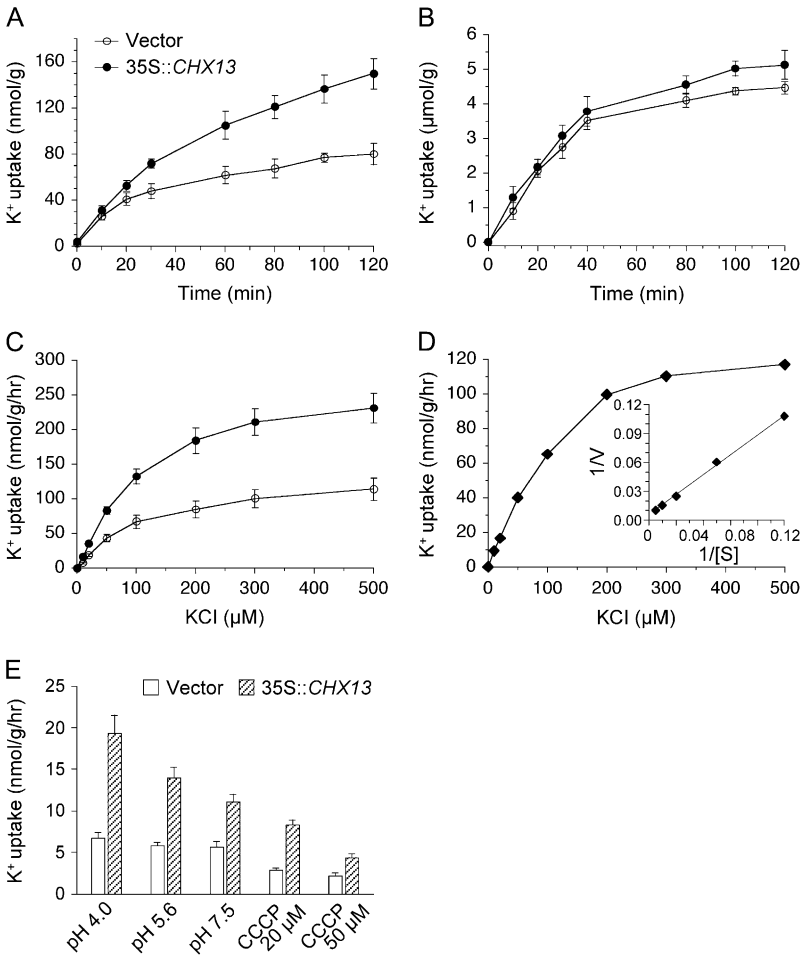

Figure 7. K^+ ($^{86}Rb^+$) uptake in plants overexpressing *AtCHX13*. Seven-day-old seedlings grown hydroponically in B5 medium were washed and transferred to 0.5× Murashige and Skoog liquid medium without K^+ for 2 d. After this K^+ depletion, the seedling roots were used for K^+ uptake assays using an $^{86}Rb^+$ tracer. Data points represent means ± SD. At least three independent experiments were performed with duplicates for each treatment. A and B, Time course of K^+ ($^{86}Rb^+$) uptake at 0.02 (A) and at 20 (B) mM external K^+. C, Uptake of K^+ ($^{86}Rb^+$) as a function of external K^+ concentration. D, AtCHX13-mediated high-affinity K^+ uptake. The AtCHX13-dependent K^+ ($^{86}Rb^+$) uptake was obtained by subtracting the uptake in vector control from that in the 35S::*AtCHX13* seedlings. Inset (D), Lineweaver-Burk plot of AtCHX13-dependent K^+ uptake. [S], K^+ concentration (μM); V, K^+ uptake rate (nmol g^{-1} h^{-1}). E, Effects of pH and CCCP on AtCHX13-mediated K^+ ($^{86}Rb^+$) uptake at 20 μM external [K^+]. Different pH values were obtained by adjusting MES-Tris combinations. Effect of CCCP on AtCHX13-mediated K^+ uptake was tested at pH 4.3. Protonophore CCCP was added to the uptake medium 5 min prior to K^+ and Rb^{86} tracer addition. The AtCHX13-dependent K^+ uptake is compared to the uptake in vector control from that in the 35S::*AtCHX13* seedlings. Data show net uptake at 10 min.

different K^+ concentrations and varied pH, like another member of the CPA2 family from bacteria, Kef C (Booth et al., 1996). Future studies of a purified and active CHX in a reconstituted system are needed to establish the mode of transport.

Role of AtCHX13 in K^+ Nutrition

atchx13 seedlings displayed growth inhibition when grown under K^+-deficient conditions (pH 4.3; Fig. 6; Supplemental Fig. S6). Our seedling expression data confirmed expression of the transporter during K^+-limiting conditions. These results support the idea that AtCHX13 is important for K^+ acquisition when this nutrient is limited. Consistent with this idea, plants overexpressing *AtCHX13* are more tolerant to low K^+ than wild-type controls.

AtCHX13 is preferentially expressed in mature pollen grains and in elongating pollen tubes (Sze et al., 2004), but also in the roots. However, in vitro pollen tube elongation of *atchx13* lines were similar to wild type. Preliminary studies with *atchx13/14* double mutants also failed to reveal obvious differences in pollen tube growth (data not shown). Yet *atchx13* seedlings grew poorly on K^+-depleted medium compared to wild type and displayed reduced K^+ uptake at low K^+ concentrations (Supplemental Fig. S5). Wild-type roots showed little or no detectable *AtCHX13* promoter::GUS activity in roots, although K^+ starvation induced an increase in GUS activity particularly in the root tip (Fig. 4C). Expression of *AtCHX13* in wild-type roots as shown by RT-PCR (Fig. 5B) is confirmed by *AtCHX13* transcript detected in lateral root cap cells by ATH1 microarray (Birnbaum et al., 2003). Assuming AtCHX13 function is limited to the root tip of the vegetative plant body, these results would suggest that AtCHX13 could play a signaling role critical for transmitting the low K^+ signal to the rest of the plant. The root tip (including the root cap cells) can serve as a sensor of the environment (Svistoonoff et al., 2007), and AtCHX13 activity may be involved in transducing environmental signals. Mutant seedlings unable to communicate the K^+ levels in the milieu may not elicit appropriate responses and thus seedlings fail to tolerate the K^+ nutrient stress. As root tip cells express other members of the CHX family (Birnbaum et al., 2003; Padmanaban et al., 2007), it is intriguing to speculate the high-affinity K^+ uptake and the plasma membrane location of AtCHX13 give root cells the specific features needed to sense and respond to environmental stresses.

SUMMARY

AtCHX13 is the first functionally characterized CHX transporter to be localized to the plasma membrane. Using both yeast and plant expression systems, AtCHX13 facilitated high-affinity K^+ uptake when K^+ was limiting.

MATERIALS AND METHODS

Plant Materials and Growth Conditions

Arabidopsis (*Arabidopsis thaliana*) Col-0 seeds were used as wild type (control). *atchx13* T-DNA insertion mutant lines in the Col-0 ecotype were obtained by screening SALK and SAIL lines (http://signal.salk.edu). Seeds from these lines were obtained from the Arabidopsis Biological Resource Center. Two *atchx13* homozygous lines were screened from T-DNA insertion lines, SALK_095075 (*atchx13-1*) and SALK_023605 (*atchx13-2*). In both lines, the T-DNA was inserted in the last exon of the AtCHX13 ORF. PCR was used to confirm the lines contained the proper T-DNA insertion by using T-DNA primers and AtCHX13 gene-specific primers, 5′-ATGGAGCTTTCGATGTTTGGC-3′ (for SALK_023605 lines) or 5′-GAGTTTACCGAGATCAATGGTAG-3′ (for SALK_095075 lines).

Arabidopsis seeds were surface sterilized and sown on 0.5× Murashige and Skoog plates. K^+-deficient 0.5× Murashige and Skoog medium was made with KNO_3 replaced by BTP, KH_2PO_4 replaced by NaH_2PO_4, and KI replaced by NaI. The K^+ concentration in the medium was adjusted by mixing specific amounts of Murashige and Skoog medium and K^+-deficient Murashige and Skoog medium. The plates contained 0.8% agar and 1% Suc. The pH of the medium was buffered with 5 mM MES to pH 4.5, pH 5.6, and with 5 mM Tris-MES, pH 7.5.

Analyzing Growth, Biomass, and Chlorophyll Content

Arabidopsis Col-0 seeds were used as wild type. Col-0, *atchx13-1*, *atchx13-2*, and 35S::*AtCHX13* seeds were germinated on normal 0.5× Murashige and Skoog and on K^+-deficient medium and incubated in a growth chamber at 16-h-light/8-h-dark cycles at 22°C. Plant phenotypes were recorded after 3 to 4 weeks. Total chlorophyll content was extracted from seedlings with 90% acetone, and chlorophyll *a*/*b* was measured as described previously (Porra et al., 1989). Seedlings were removed and blotted dry with tissue prior to determining biomass. Biomass of plant seedlings was expressed as fresh weight per 20 seedlings.

Plasmid Construction

To isolate *AtCHX13* cDNA, total RNA was isolated from mature pollen grains of Arabidopsis (Col-0) plants by the guanidine/acid-phenol method (Sze et al., 2004). The first-strand cDNA was synthesized using reverse transcriptase. Primers X13Cf (5′-GGGGACAAGTTTGTACAAAAAAGCAGGCTTTACTGATAAGGAAAAGACTATGGAGCT-3′) and X13Cr (5′-GGGGACCACTTTGTACAAGAAAGCTGGGTCAATGGTAGTGAAACCTTCTTCAGCA-3′) were used to amplify the *AtCHX13* cDNA by PCR (25 cycles, 94°C 30 s, 55°C 30 s, and 72°C 90 s). The forward and reverse primers contain attB1 and attB2 sequences for Gateway recombination cloning. Gel-purified PCR products were recombined with pDONR221 using BP clonase, according to the manufacturer's instructions (Invitrogen). Resulting clones were sequenced using forward and reverse M13 primers and gene-specific primers X13s1f (5′-GTCATCCATCTCTTCCTCCT-3′), X13s2f (5′-CTATAGCTAGCCTTAGTGGA-3′), X13s3f (5′-GTGGTGTACCTCTACGACCCT-3′), and X13s4f (5′-CGTGATTCCGTTCCACAAGCA-3′). The correctly spliced clone containing the longest ORF was named as entry clone pECHX13. After the initial cloning, *AtCHX13* was amplified using forward primer 5′-GGATCCATGGAGCTTTCGATGTTTGGCAGAG (*Bam*HI site underlined) and reverse primer 5′-CGCGGCCGCCTAGCGTTTACCGAGATCAATGGTAGTGAAACCTTC (*Not*I site underlined).

The resulting cDNA fragment was cloned into yeast (*Saccharomyces cerevisiae*) expression vector pUGpd, using the GPD promoter to express the GFP-tagged AtCHX13, and was made using PCR. The *AtCHX13* cDNA was amplified by using the following primers for PCR: 5′-GGTACCACTAGTATGGAGCTTTCGATGTTTGGCAGAG-3′ (*Eco*RI and *Spe*I sites underlined) and CHX13-GFP3, 5′-GCGGCCGCGCGTTTACCGAGATCAATGGTAGTGAAACCTTCT-3′ (*Not*I site underlined). The PCR product was sequenced and ligated into the yeast pUGpd-GFP vector at *Spe*I and *Not*I sites. The resulting constructs contained the AtCHX13 reading frame fused to the 5′ of the GFP ORF. The clone was confirmed by sequencing and introduced into yeast.

Constructs for Plant Expression

Plant transient expression constructs were generated by PCR amplification using the yeast *AtCHX13-GFP* plasmid DNA as a template. *AtCHX13-GFP* was amplified with a forward primer, 5′-GCGGCCAAATCGGCCATGGAGCTTTCGATGTTTGGCAGAG-3′ (*Sfi*IA), and a reverse primer, 5′-CGGGCCCTTATGGCCTAATAACTTGTACAGCTCGTCCAT-3′ (*Sfi*IB). The AtCHX13-GFP fusion was inserted into a transient expression vector pRTL1 at the *Sfi*I site. Resulting construct harbored the cauliflower mosaic virus 35S promoter driving *AtCHX13-GFP* followed by the NOS terminator. The plasmid was used for both transient expression in onion (*Allium cepa*) and tobacco (*Nicotiana tabacum*) epidermal cells.

Stable 35S::*AtCHX13* constructs for expression in plants were generated by recombination cloning as described previously (Clough and Bent, 1998; Sze et al., 2004; Shigaki et al., 2005). The third generation of Basta-resistant lines was verified by RT-PCR analysis.

Gene Expression Analysis by Northern Blot, RT-PCR, and Promoter-Driven GUS Activity

For RNA analysis, Col-0 seeds were germinated in soil (Metro-Mix 360) and grown under continuous light. Two-week-old seedlings were washed with water and then floated in the metal-containing medium for 16 h. RNA was extracted from tissues using an RNeasy kit (Qiagen). Ten micrograms of total RNA was used for northern-blot analysis as described previously.

For RT-PCR analysis, 4-week-old Col-0 seedlings were used. For K^+ stress treatment, Col-0 seedlings were grown on 0.5× Murashige and Skoog for 1 week under 16-h-light/8-h-dark cycles, then transferred to K^+-deficient plates (0 or 2 mM K^+) and K^+-containing plates (50 mM K^+ and 100 mM K^+). Whole seedlings were harvested daily to monitor gene expression. Total RNA was isolated from root, leaf, flower, and siliques of Arabidopsis using an RNeasy kit (Qiagen). First-strand cDNA was synthesized with a Superscript II RNase H^- reverse transcriptase kit using oligo$(dT)_{12-18}$ as primer (Invitrogen), according to the manufacturer's instructions. PCR was performed with the following program: 94°C for 2 min to denature DNA, followed by 30 cycles of 94°C (30 s), 58°C (30 s), and 72°C (60 s), followed by 72°C for 10-min extension. ACTIN1 was used as control. ACTIN1: forward primer, 5′-GTGCTCGACTCTGGAGATGGTGTG-3′ and reverse primer, 5′-CGGCGATTCCAGGGAACATTGTGG-3′; AtCHX13 forward primer P1, 5′-GACTAGTCTTTACGCGCTTTCCATG-3′ and reverse primer P2, 5′-TATGTCGTTGTTTATACTCGAGTAAGGCG-3′.

AtCHX13::GUS reporter lines were generated as described previously (Sze et al., 2004) and seeds were germinated on 0.5× Murashige and Skoog agar plates (10 mM K^+) for 1 week, and then seedlings were transferred to K^+-depleted plates (0 mM K^+) or K^+ stress (50 mM K^+ and 100 mM K^+) conditions. Seedlings were harvested regularly to monitor GUS expression. GUS staining was conducted as described previously (Sze et al., 2004). Samples were photographed using a Nikon (Tokyo) E600W microscope.

Particle Bombardment of Plant Cells and Confocal Microscopy

Five micrograms of plasmid DNA containing the 35S::*GFP*, 35S::*AtCHX13-GFP* was mixed with 20 μL of an aqueous suspension containing 1.6-μm gold particles. The gold DNA suspensions were vortexed in the presence of $CaCl_2$ and spermidine and incubated on ice. After centrifugation, the plasmid-coated gold particles were washed and resuspended in ethanol. The gold was spread onto plastic carrier discs for biolistic bombardment of tobacco and onion epidermal cells using a Bio-Rad 1000/HE particle delivery system. After 12 to 15 h, GFP from the epidermal cells of tobacco leaves and onion were imaged with a Leica TCS SP2 AOBS laser confocal scanning microscope (Leica Microsystems). GFP was excited with the 488-nm line of the argon laser and emission was detected at 520 nm.

Transport K^+ (^{86}Rb) Uptake into Plant

To characterize the K^+-transport activities of AtCHX13, ^{86}Rb tracer experiment was performed (Wu et al., 1996; Rigas et al., 2001). The $^{86}RbCl$ salt with a specific activity of 7.85 mCi/mg was purchased from Perkin-Elmer (Life and Analytical Sciences). Plants were grown hydroponically for 7 d in sterile flasks on B5 medium, 2% Suc, and 0.05% MES, pH 5.7. Seedlings were harvested and preincubated for 2 d in K^+-free Murashige and Skoog medium. $^{86}Rb^+$ uptake assays were conducted in K^+-free Murashige and Skoog medium buffered with 5 mM MES to pH 5.0, supplemented with 0.5 μCi ^{86}Rb and various concentrations of KCl (0.02 or 20 mM). Samples (about six seedlings) were taken at 10, 20, 30, 60, 80, 100, and 120 min, respectively, washed with 3×10 mL of K^+-free Murashige and Skoog medium, and then placed for 20 min in 40 mL of ice-cold K^+-free Murashige and Skoog medium. Subsequently, the seedlings were blotted on filter paper, weighed, and activity measured using a scintillation counter.

For kinetic analysis, seedlings were incubated in various external K^+ concentrations (10, 20, 50, 100, 200, 300, 500 μM) for 10 min. Different pH values of uptake buffer containing 2% Suc were obtained by adjusting MES-Tris combinations. Uptake lasted for 10 min and then samples were washed as described above for radioactivity counting.

Yeast Strains, Medium, and Growth Conditions

Yeast strains LMM04 (ade2-1 can1-100 his3-11,15 leu2-3,112 trp1-1 ura3-1 mall0 ena1Δ::HIS3::ena4Δ nha1Δ::LEU2 trk1Δ::LEU2 trk2Δ::HIS3 kha1Δ::kanMX:tok1Δ) and 59m15 (trk1::LEU2 trk2::HIS3) were used to characterize AtCHX13 (Madrid et al., 1998; Maresova and Sychrova, 2005). LMM04 or 59m15 cells expressing AtCHX13, AtKAT1, or empty vector were grown in SC-Ura medium containing 100 mM KCl at 30°C overnight. Five-fold serial dilutions were prepared from the saturated yeast cultures and 3-μL aliquots of each dilution were spotted on SC-Ura plates with or without various concentrations of KCl under different pH conditions (Maresova and Sychrova, 2005). The pH of SC medium was adjusted with 5 mM MES for pH 4.5 and 6.0 and 5 mM Tris-Cl buffer for pH 7.5. Plates were incubated at 30°C for 4 d.

Yeast cation analysis was performed as described previously (Eide et al., 2005; Mei et al., 2007). Yeast LMM04 cells expressing *AtCHX13*, *AtKAT1*, and empty vector were grown overnight in 5 mL SC-Ura medium supplemented with 100 mM KCl. After rinsing and diluting with K^+-free SC-Ura medium, 100 μL of yeast cells were inoculated into 5 mL fresh SC-Ura medium supplemented with 5 mM K^+ and grown at 30°C overnight. About 2.5 mL of the yeast cultures were collected by vacuum filtration using isopore membrane filters (1.2-μm pore size; Fisher Scientific). Cells were washed three times with 1 mL of 1 μM ethylenediaminetetraacetic acid disodium salt solution, pH 8.0, followed by three washes with 1 mL of deionized water. The filters were dried in a 70°C oven for 48 h for inductively coupled plasma-mass spectroscopy analysis (Lahner et al., 2003).

For observation of AtCHX13-GFP signals, the yeast harboring the AtCHX13-GFP fusion were grown in SC-His-Leu medium overnight. The yeast cells were viewed under laser-scanning confocal microscope (Olympus Fluoview, FV 500; Olympus Optical). An argon laser beam was used for excitation at 488 nm and GFP visualization with emission at 525 nm.

Transport in Yeast

To characterize the K^+ transport activities of AtCHX13 in yeast, K^+ uptake using $^{86}Rb^+$ as tracer was performed (Fu and Luan, 1998; Rubio et al., 1999). LMM04 yeast cells expressing vector, *AtCHX13*, and *AtKAT1* were grown to midlog phase in the Ura-deficient SC medium containing 50 mM KCl. Cells were harvested and washed and K^+ starved in low-salt Arg-P medium (Rodriguez-Navarro and Ramos, 1984) for 5 h before the uptake assay. For the time course study, 5×10^8 cells were added to 50 mL of the uptake solution (pH 4.5) containing 0.5 μCi $^{86}Rb^+$/mL and 0.02 and 20 mM KCl in culture flasks and gently shaken. A fraction of the cells was harvested at the indicated times. For kinetic studies, 10^7 cells were used in each uptake sample in a 1-mL solution containing 0.5 μCi $^{86}Rb^+$ and various concentrations of KCl. The $^{86}Rb^+$ radioactivity taken up into the cells was measured by a liquid scintillation counter (model LS6000IC; Beckman Instruments). To test whether other cations reduced K^+ uptake, 0, 0.1, 0.2, 0.5, 1, 5, 10, 20, or 100 mM NaCl or CsCl was included in the uptake assay reaction containing 0.02 mM KCl. For comparison of Rb^+ and K^+ affinity, $^{86}Rb^+$ uptake in the standard reaction plus nonradioactive K^+ or Rb^+ at 0.02, 2.0, and 20 mM was conducted. The different pH of the uptake medium containing 10 mM Glc was adjusted using 5 mM MES or Tris. Effect of Glc on AtCHX13-mediated K^+ uptake was tested by comparison of uptake in 10 mM Glc with that after depletion of 10 mM Glc from uptake buffer under pH 4.5. Protonophore CCCP was added to the yeast cells in uptake medium (pH 4.5) 5 min prior to K^+ and ^{86}Rb tracer addition. After 5 min of uptake, samples were filtered and washed with 10 mM RbCl for scintillation counting. All uptake experiments were performed in duplicate with three independent replicates (unless otherwise noted).

Sequence data from this article can be found in the GenBank/EMBL data libraries under accession number EF571901.

Supplemental Data

The following materials are available in the online version of this article.

Supplemental Figure S1. AtCHX13 is similar to other Arabidopsis CHX transporters.

Supplemental Figure S2. Functional expression of *AtCHX13* in yeast mutant 59m15.

Supplemental Figure S3. GFP-tagged AtCHX13 functions in yeast suppression assays.

Supplemental Figure S4. Phenotyping *atchx13* mutants and overexpression transgenic lines.

Supplemental Figure S5. K^+ ($^{86}Rb^+$) uptake in seedlings of *chx13* mutants.

Received June 9, 2008; accepted July 29, 2008; published August 1, 2008.

LITERATURE CITED

Anderson JA, Huprikar SS, Kochian LV, Lucas WJ, Gaber RF (1992) Functional expression of a probable Arabidopsis thaliana potassium channel in Saccharomyces cerevisiae. Proc Natl Acad Sci USA **89:** 3736–3740

Birnbaum K, Shasha DE, Wang JY, Jung JW, Lambert GM, Galbraith DW, Benfey PN (2003) A gene expression map of the Arabidopsis root. Science **302:** 1956–1960

Bock KW, Honys D, Ward JM, Padmanaban S, Nawrocki EP, Hirschi KD, Twell D, Sze H (2006) Integrating membrane transport with male gametophyte development and function through transcriptomics. Plant Physiol **140:** 1151–1168

Booth IR, Jones MA, McLaggan D, Nikolaev Y, Ness LS, Wood CM, Miller S, Tötemeyer S, Ferguson GP (1996) Bacterial ion channels. *In* WN Konings, HR Kaback, JS Lolkema, eds, Transport Processes in Eukaryotic and Prokaryotic Organisms, Vol 2. Elsevier Press, New York, pp 693–729

Cellier F, Conéjéro G, Ricaud L, Luu DT, Lepetit M, Gosti F, Casse F (2004) Characterization of AtCHX17, a member of the cation/H^+ exchangers, CHX family, from Arabidopsis thaliana suggests a role in K^+ homeostasis. Plant J **39:** 834–846

Clough S, Bent A (1998) Floral dip: a simplified method for Agrobacterium-mediated transformation of Arabidopsis thaliana. Plant J **16:** 735–743

Eide DJ, Clark S, Nair TM, Gehl M, Gribskov M, Guerinot ML, Harper JF (2005) Characterization of the yeast ionome: a genome-wide analysis of nutrient mineral and trace element homeostasis in Saccharomyces cerevisiae. Genome Biol **6:** R77

Elumalai RP, Nagpal P, Reed JW (2002) A mutation in the *Arabidopsis* KT2/KUP2 potassium transporter gene affects shoot cell expansion. Plant Cell **14:** 119–131

Epstein E (1972) Mineral Nutrition of Plants: Principles and Perspectives. John Wiley and Sons, New York

Fu HH, Luan S (1998) AtKUP1: a dual-affinity K^+ transporter from *Arabidopsis*. Plant Cell **10:** 63–73

Fukada-Tanaka S, Inagaki Y, Yamaguchi T, Saito N, Iida S (2000) Colour-enhancing protein in blue petals. Nature **407:** 581–582

Gaymard F, Pilot G, Lacombe B, Bouchez D, Bruneau D, Boucherez J, Michaux-Ferrière N, Thibaud JB, Sentenac H (1998) Identification and

disruption of a plant shaker-like outward channel involved in K^+ release into the xylem sap. Cell **94:** 647–655

Hall D, Evans AR, Newbury HJ, Pritchard J (2006) Functional analysis of CHX21: a putative sodium transporter in Arabidopsis. J Exp Bot (Special Issue) **57:** 1201–1210

Hedrich R, Schroeder JI (1989) The physiology of ion channels and electrogenic pumps in higher plants. Annu Rev Plant Physiol Plant Mol Biol **40:** 539–569

Kim EJ, Kwak JM, Uozumi N, Schroeder JI (1998) AtKUP1: an *Arabidopsis* gene encoding high-affinity potassium transport activity. Plant Cell **10:** 51–62

Kochian LV, Garvin DF, Shaff JE, Chilcott TC, Lucas WJ (1993) Towards an understanding of the molecular basis of plants K^+ transport: characterization of cloned K^+ transport cDNAs. Plant Soil **155/156:** 115–118

Lahner B, Gong J, Mahmoudian M, Smith EL, Abid KB, Rogers EE, Guerinot ML, Harper JF, Ward JM, McIntyre L, et al (2003) Genomic scale profiling of nutrient and trace elements in Arabidopsis thaliana. Nat Biotechnol **21:** 1215–1221

Lebaudy A, Very AA, Sentenac H (2007) K^+ channel activity in plants: genes, regulations and functions. FEBS Lett **581:** 2357–2366

Madrid R, Gómez MJ, Ramos J, Rodríguez-Navarro A (1998) Ectopic potassium uptake in trk1 trk2 mutants of Saccharomyces cerevisiae correlates with a highly hyperpolarized membrane potential. J Biol Chem **273:** 14838–14844

Maresova L, Sychrova H (2005) Physiological characterization of Saccharomyces cerevisiae kha1 deletion mutants. Mol Microbiol **55:** 588–600

Maresova L, Sychrova H (2006) Yeast functional analysis report. Arabidopsis thaliana CHX17 gene complements the kha1 deletion phenotypes in Saccharomyces cerevisiae. Yeast **23:** 1167–1171

Marschner H (1995) Mineral Nutrition of Higher Plants, Ed 2. Academic Press, San Diego

Maser P, Thomine S, Schroeder JI, Ward JM, Hirschi K, Sze H, Talke IN, Amtmann A, Maathuis FJ, Sanders D, et al (2001) Phylogenetic relationships within cation transporter families of Arabidopsis. Plant Physiol **126:** 1646–1667

Mei H, Zhao J, Pittamn J, Lachmansingh J, Park S, Hirschi KD (2007) In planta regulation of the Arabidopsis Ca^{2+}/H^+ antiporter CAX1. J Exp Bot **12:** 3419–3427

Nakamura RL, Anderson JA, Gaber RF (1997) Determination of key structural requirements of a K^+ channel pore. J Biol Chem **272:** 1011–1018

Padmanaban S, Chnroj S, Kwak JM, Li X, Ward J, Sze H (2007) Participation of endomembrane cation/H^+ exchanger AtCHX20 in osmoregulation of guard cells. Plant Physiol **44:** 82–93

Pardo JM, Cubero B, Leidi EO, Quintero FJ (2006) Alkali cation exchangers: roles in cellular homeostasis and stress tolerance. J Exp Bot **57:** 1181–1199

Porra RJ, Thompson WA, Kriedemann PE (1989) Determination of accurate extinction coefficients and simultaneous equations for assaying chlorophylls a and b extracted with four different solvents: verification of the concentration of chlorophyll standards by atomic absorption spectroscopy. Biochim Biophys Acta **975:** 384–394

Rigas S, Debrosses G, Haralampidis K, Vicente-Agullo F, Feldmann KA, Grabov A, Dolan L, Hatzopoulos P (2001) TRH1 encodes a potassium transporter required for tip growth in *Arabidopsis* root hairs. Plant Cell **13:** 139–151

Rodriguez-Navarro A, Ramos J (1984) Dual system for potassium transport in Saccharomyces cerevisiae. J Bacteriol **159:** 940–945

Rodriguez-Navarro A, Rubio F (2006) High-affinity potassium and sodium transport systems in plants. J Exp Bot **57:** 1149–1160

Rubio F, Schwarz M, Gassmann W, Schroeder JI (1999) Genetic selection of mutations in the high affinity K^+ transporter HKT1 that define functions of a loop site for reduced Na^+ permeability and increased Na^+ tolerance. J Biol Chem **274:** 6839–6847

Schroeder JI, Ward JM, Gassmann W (1994) Perspectives on the physiology and structure of inward-rectifying K^+ channels in higher plants: biophysical implications for K^+ uptake. Annu Rev Biophys Biomol Struct **23:** 441–471

Shigaki T, Kole M, Ward JM, Sze H, Hirschi KD (2005) Cre-loxP recombination vectors for the expression of Riken Arabidopsis full-length cDNAs in plants. Biotechniques **39:** 301–302

Song CP, Guo Y, Qiu Q, Lambert G, Galbraith DW, Jagendorf A, Zhu JK (2004) A probable $Na^+(K^+)/H^+$ exchanger on the chloroplast envelope functions in pH homeostasis and chloroplast development in Arabidopsis thaliana. Proc Natl Acad Sci USA **101:** 10211–10216

Svistoonoff S, Creff A, Reymond M, Sigoillot-Claude C, Ricaud L, Blanchet A, Nussaume L, Desnos T (2007) Root tip contact with low-phosphate media reprograms plant root architecture. Nat Genet **39:** 792–796

Sze H, Padmanaban S, Cellier F, Honys D, Cheng NH, Bock KW, Conéjéro G, Li X, Twell D, Ward JM, et al (2004) Expression patterns of a novel AtCHX gene family highlight potential roles in osmotic adjustment and K^+ homeostasis in pollen development. Plant Physiol **136:** 2532–2547

Tester M (1990) Plant ion channels: whole cell and single channel studies. New Phytol **114:** 305–340

Venema K, Quintero FJ, Pardo JM, Donaire JP (2002) The Arabidopsis Na^+/H^+ exchanger AtNHX1 catalyzes low affinity Na^+ and K^+ transport in reconstituted liposomes. J Biol Chem **277:** 2413–2418

Very AA, Sentenac H (2003) Molecular mechanisms and regulation of K^+ transport in higher plants. Annu Rev Plant Biol **54:** 575–603

Ward JM (2001) Identification of novel families of membrane proteins from the model plant Arabidopsis thaliana. Bioinformatics **17:** 560–563

Wu SJ, Ding L, Zhu JK (1996) SOS1, a genetic locus essential for salt tolerance and potassium acquisition. Plant Cell **8:** 617–627